High resolution ^{80}Se(n,γ) cross section measurement at CERN n_TOF

V. Babiano-Suarez[1], J. Balibrea-Correa[1], L. Caballero-Ontanaya[1], C. Domingo-Pardo[1], I. Ladarescu[1], J. Lerendegui-Marco[2], J. L. Tain[1], F. Calviño[18], A. Casanovas[18], A. Tarifeño-Saldivia[18], C. Guerrero[2], O. Aberle[3], V. Alcayne[4], S. Amaducci[5,6], J. Andrzejewski[7], L. Audouin[8], M. Bacak[3,9,10], M. Barbagallo[3,11], S. Bennett[12], E. Berthoumieux[10], J. Billowes[12], D. Bosnar[13], A. Brown[14], M. Busso[15,16], M. Caamaño[17], M. Calviani[3], D. Cano-Ott[4], F. Cerutti[3], E. Chiaveri[3,12], N. Colonna[11], G. Cortés[18], M. A. Cortés-Giraldo[2], L. Cosentino[5], S. Cristallo[15,19], L. A. Damone[11,20], P. J. Davies[12], M. Diakaki[21,3], M. Dietz[22], R. Dressler[23], Q. Ducasse[24], E. Dupont[10], I. Durán[17], Z. Eleme[25], B. Fernández-Domínguez[17], A. Ferrari[3], P. Finocchiaro[5], V. Furman[26], K. Göbel[27], R. Garg[22], A. Gawlik-Ramięga[7], S. Gilardoni[3], I. F. Gonçalves[28], E. González-Romero[4], F. Gunsing[10], H. Harada[29], S. Heinitz[23], J. Heyse[30], D. G. Jenkins[14], A. Junghans[31], F. Käppeler[32], Y. Kadi[3], A. Kimura[29], I. Knapová[33], M. Kokkoris[21], Y. Kopatch[26], M. Krtička[33], D. Kurtulgil[27], C. Lederer-Woods[22], H. Leeb[9], S. J. Lonsdale[22], D. Macina[3], A. Manna[34,35], T. Martínez[4], A. Masi[3], C. Massimi[34,35], P. Mastinu[36], M. Mastromarco[3], E. A. Maugeri[23], A. Mazzone[11,37], E. Mendoza[4], A. Mengoni[38], V. Michalopoulou[21,3], P. M. Milazzo[39], F. Mingrone[3], J. Moreno-Soto[10], A. Musumarra[5,40], A. Negret[41], R. Nolte[24], F. Ogállar[42], A. Oprea[41], N. Patronis[25], A. Pavlik[43], J. Perkowski[7], L. Persanti[11,15,19], C. Petrone[41], E. Pirovano[24], I. Porras[42], J. Praena[42], J. M. Quesada[2], D. Ramos-Doval[8], T. Rauscher[44,45], R. Reifarth[27], D. Rochman[23], Y. Romanets[28], C. Rubbia[3], M. Sabaté-Gilarte[2,3], A. Saxena[46], P. Schillebeeckx[30], D. Schumann[23], A. Sekhar[12], A. G. Smith[12], N. V. Sosnin[12], P. Sprung[23], A. Stamatopoulos[21], G. Tagliente[11], L. Tassan-Got[3,21,8], Th. Thomas[27], P. Torres-Sánchez[42], A. Tsinganis[3], J. Ulrich[23], S. Urlass[31,3], S. Valenta[33], G. Vannini[34,35], V. Variale[11], P. Vaz[28], A. Ventura[34], D. Vescovi[15], V. Vlachoudis[3], R. Vlastou[21], A. Wallner[47], P. J. Woods[22], T. Wright[12], and P. Žugec[13]
and the n_TOF Collaboration

[1]Instituto de Física Corpuscular, CSIC - Universidad de Valencia, Spain
[2]Universidad de Sevilla, Spain
[3]European Organization for Nuclear Research (CERN), Switzerland
[4]Centro de Investigaciones Energéticas Medioambientales y Tecnológicas (CIEMAT), Spain
[5]INFN Laboratori Nazionali del Sud, Catania, Italy
[6]Dipartimento di Fisica e Astronomia, Università di Catania, Italy
[7]University of Lodz, Poland
[8]Institut de Physique Nucléaire, CNRS-IN2P3, Univ. Paris-Sud, Université Paris-Saclay, F-91406 Orsay Cedex, France
[9]TU Wien, Atominstitut, Stadionallee 2, 1020 Wien, Austria
[10]CEA Irfu, Université Paris-Saclay, F-91191 Gif-sur-Yvette, France
[11]Istituto Nazionale di Fisica Nucleare, Sezione di Bari, Italy
[12]University of Manchester, United Kingdom
[13]Department of Physics, Faculty of Science, University of Zagreb, Zagreb, Croatia
[14]University of York, United Kingdom
[15]Istituto Nazionale di Fisica Nucleare, Sezione di Perugia, Italy
[16]Dipartimento di Fisica e Geologia, Università di Perugia, Italy
[17]University of Santiago de Compostela, Spain
[18]Universitat Politècnica de Catalunya, Spain
[19]Istituto Nazionale di Astrofisica - Osservatorio Astronomico di Teramo, Italy
[20]Dipartimento Interateneo di Fisica, Università degli Studi di Bari, Italy
[21]National Technical University of Athens, Greece
[22]School of Physics and Astronomy, University of Edinburgh, United Kingdom
[23]Paul Scherrer Institut (PSI), Villigen, Switzerland
[24]Physikalisch-Technische Bundesanstalt (PTB), Bundesallee 100, 38116 Braunschweig, Germany
[25]University of Ioannina, Greece
[26]Joint Institute for Nuclear Research (JINR), Dubna, Russia
[27]Goethe University Frankfurt, Germany
[28]Instituto Superior Técnico, Lisbon, Portugal
[29]Japan Atomic Energy Agency (JAEA), Tokai-Mura, Japan
[30]European Commission, Joint Research Centre (JRC), Geel, Retieseweg 111, B-2440 Geel, Belgium
[31]Helmholtz-Zentrum Dresden-Rossendorf, Germany
[32]Karlsruhe Institute of Technology, Campus North, IKP, 76021 Karlsruhe, Germany
[33]Charles University, Prague, Czech Republic

[34]Istituto Nazionale di Fisica Nucleare, Sezione di Bologna, Italy
[35]Dipartimento di Fisica e Astronomia, Università di Bologna, Italy
[36]Istituto Nazionale di Fisica Nucleare, Sezione di Legnaro, Italy
[37]Consiglio Nazionale delle Ricerche, Bari, Italy
[38]Agenzia nazionale per le nuove tecnologie (ENEA), Bologna, Italy
[39]Istituto Nazionale di Fisica Nucleare, Sezione di Trieste, Italy
[40]Dipartimento di Fisica e Astronomia, Università di Catania, Italy
[41]Horia Hulubei National Institute of Physics and Nuclear Engineering, Romania
[42]University of Granada, Spain
[43]University of Vienna, Faculty of Physics, Vienna, Austria
[44]Department of Physics, University of Basel, Switzerland
[45]Centre for Astrophysics Research, University of Hertfordshire, United Kingdom
[46]Bhabha Atomic Research Centre (BARC), India
[47]Australian National University, Canberra, Australia

Abstract. Neutron capture cross section measurements of isotopes close to *s*-process branching-points are of fundamental importance for the understanding of this nucleosynthesis mechanism through which about 50% of the elements heavier than iron are produced. We present in this contribution the results corresponding to the high resolution measurement, for first time ever, of the ^{80}Se(n, γ) cross section, in which 98 resonances never measured before have been reported. As a consequence, ten times more precise values for the MACS have been obtained compared to previous accepted value adopted in the astrophysical KADoNiS data base.

1 Introduction

The formation of elements more massive than iron in the universe is carried out mainly by two different nucleosynthesis processes that take place inside stars [1, 2]. This work contributes to the study of one of them, the slow (*s*-) neutron capture or *s*-process, in which new elements are produced after a sequence of neutron captures and β-decays. The production of elements with mass A > 90 is ascribed to the *main* component of the *s*-process, which occurs in low mass stars (M < 3M$_\odot$) during their Asymptotic Giant Branch (AGB) evolutionary stage. There, neutrons are produced by the ^{13}C(α, n)^{16}O and ^{22}Ne(α, n)^{25}Mg reactions corresponding to the H-burning phase [3] (see Tab. 1). The *weak* component, on the other hand, is responsible for the formation of elements in the mass range 60 < A < 90. This component of the *s*-process occurs in Massive Stars during the He-burning and C-burning phases, where the ^{22}Ne(α, n)^{25}Mg and ^{12}C(^{12}C, n)^{23}Mg reactions are the neutron sources [3] (see Tab. 2).

Table 1. Summary of the *s*-process conditions in AGB stars.

Stage	He-flash	^{13}C-pocket
Neutron seed	^{22}Ne(α, n)^{25}Mg	^{13}C(α, n)^{16}O
N. density (cm^{-3})	10^9 - 10^{11}	10^7
kT (keV)	23	8

Table 2. Summary of the *s*-process conditions in massive stars.

Stage	He-burning	C-burning
Neutron seed	^{22}Ne(α, n)^{25}Mg	^{12}C(^{12}C, n)^{23}Mg [3]
N. density (cm^{-3})	< 10^6	10^{11}
kT (keV)	26	90

The relatively low neutron densities reached during the *s*-process (see Tab. 1 and Tab. 2) allow the β-decay of the possible unstable nuclei formed, and keep the *s*-process path always close to the stability valley of the nuclear chart. Furthermore, the abundances of elements along this path can be estimated by the hydrodynamic stellar models [4, 5] and post-processing tools [6, 7], which are able to simulate the lifespan of a star and estimate the abundance ratios provided by the *s*-process.

Along the *s*-process path, some long-lived nuclei divide the nucleosynthesis flow. In these branching points, the final route followed by the *s*-process depends on the physical conditions of the stellar media. One of the more relevant *s*-process branching points is ^{79}Se [8] ($t_{1/2}$ = 3 × 10^5 y [9]), which exhibits quantum states at low excitation energies that can be populated at thermal energies of the star. Since the strength of the β-decay depends on the levels involved in the transitions, the half-life of this nucleus will depend on the temperature of the star. In addition, the abundance of the *s*-only isotopes of Krypton, ^{80,82}Kr, has been accurately measured in bulk SiC acid residues [10]. Hence, comparing these experimental abundances to those predicted by the stellar models can place constraints on the astrophysical conditions of the *s*-process. To this aim, the neutron capture cross section and the β-decay rates of all isotopes involved in this branching become the experimental input for the stellar models.

In this work, we present the first high resolution neutron capture cross section measurement of ^{80}Se using the Time-of-Flight (ToF) technique. This measurement was carried out at CERN n_TOF [11] under the framework of the ERC-funded project HYMNS [12]. While there exists a previous measurement on the ^{80}Se(n, γ) cross section that employs the same technique [13], it suffers from a limited resolution and a 3 keV low energy cutoff. Due to the former, no resonance structures can be appreciated in these results. On the other hand, the lack of low-energy data prevented the study of this region so relevant for the *s*-process. These drawbacks have been

overcome in the present work, in which the ^{80}Se(n, γ) cross section has been obtained with high resolution in the entire energy range of astrophysical interest between 1 eV and 100 keV.

2 Experimental setup at CERN n_TOF

A high luminosity pulsed neutron beam is available at the neutron time of flight facility n_TOF, within the CERN accelerator complex, when approximately 7×10^{12} protons impinge onto a massive lead target producing $\sim$ 300 neutrons per proton by means of spallation reactions [14]. A 4 cm thick layer of borated water, acting as a moderator, allows one to obtain a white neutron spectrum covering the entire range of astrophysical interest between meV to MeV in one single experiment. After the application of high intense magnetic fields, mostly non-charged particles, such as neutrons, travel through the L = 185 m long tunnel that separates the spallation target and the EAR1 experimental area. The time of flight t_{ToF} of neutrons is measured to compute their kinetic energy by applying Eq. 1, where L and t_{ToF} are introduced in m and μs to obtain E_n in eV. Apart from neutrons, γ-rays generated during spallation reactions arrive to EAR1 as a high intense pulse known as γ-flash. The saturated electrical signal coming from the detection of this pulse determines the origin of the time in the calculation of t_{ToF}.

$$E_n = \left(\frac{72.2977L}{t_{ToF}}\right)^2 \quad (1)$$

Four scintillation C_6D_6 detectors were placed at EAR1 to detect the prompt γ-ray radiation coming from neutron captures. The fast response of the C_6D_6 organic scintillation liquid allows us to obtain a high resolution measurement on the neutron kinetic energy. In addition, the low neutron sensitivity of the complete detector reduces the background due to neutron captured in the structural material or within the detection volume itself [15, 16]. Fig. 1 shows two of these detectors, all of them placed 125° from the beam line to minimize the impact of anisotropic emission of the primary γ-rays for capture events with $l > 0$ [17]. This figure also displays the four disk-shaped samples of 20 mm diameter measured during the experimental campaign, attached to a sample exchanger device that allows the user to remotely switch them. In addition to the ^{80}Se sample of 2.965(5) g of mass, 3.50(5) mm thick and 99.9(1)% purity, dummy and lead samples were measured to estimate different background components. Furthermore, a gold sample was measured to normalize the ^{80}Se capture yield by means of the saturated resonance method (SRM) [18].

3 Data analysis

Neutrons arriving to the experimental hall can be captured in the sample by emitting a random number of γ-rays only constrained by their total energy, E_C, which is approximately equal to the sum of the neutron separation

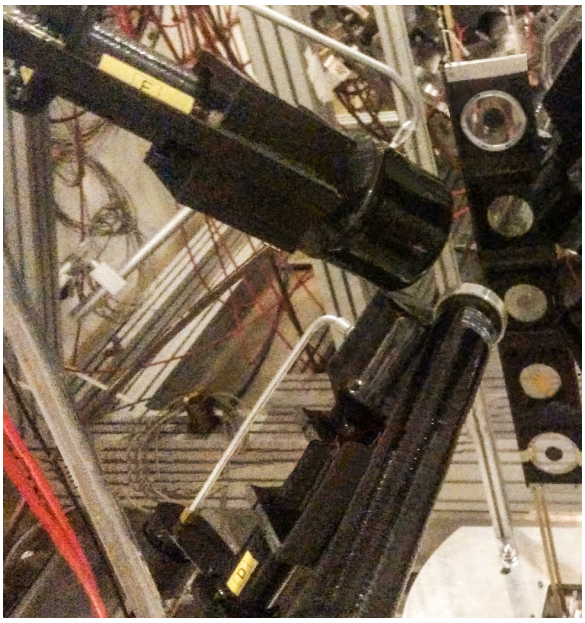

Figure 1. Picture of two out of the four C_6D_6 detectors mounted in EAR1 for the ^{80}Se(n, γ) cross section experiment.

energy, S_n, and the energy of the incoming neutron, E_n ($E_C \approx S_n + E_n$). The fraction of incoming neutrons that are captured in the sample is known as the capture yield, Y, and it can be obtained by means of Eq. 2. In the latter, N_n is the number of incoming neutrons and N the number of detected γ-rays that have been generated by neutron captures in the sample and deposit an energy E_{dep} in the detector.

$$Y(E_n) = \frac{N(E_n, E_{dep})}{N_n(E_n)\varepsilon(E_{dep})} \quad (2)$$

All background components must be subtracted to obtain a correct value of the ^{80}Se capture yield. In this work, we have directly measured the background components related to the ambient (beam-off) radiation, and those γ-rays generated by neutrons scattered and captured in the surroundings of the experimental setup. The background components related to the scattering of in-beam γ-rays and neutrons in the ^{80}Se sample, have been estimated by performing ancillary measurements.

However, the main experimental challenge here is related to the detection efficiency ε, which depends on the deposited energy and number of γ-rays in the generated cascade. This makes the measured counting rate dependent from the multiplicity of the cascade, which results in an incorrect determination of the capture yield. To overcome this challenge, the Pulse Height Weighting Technique (PHWT) has been employed in this work [19]. Monte Carlo (MC) simulations of the entire experimental setup were carried out using the based C++ Geant4 toolkit [20, 21] in order to obtain a Weighting Function (WF) transforming the detection efficiency of C_6D_6 proportional to the energy of the detected γ-ray. This condition, together with a small detection efficiency, ensuring to detect at most one γ-ray per capture event, transform the energy efficiency dependency of the (n,γ)

cascade to an almost constant value equal to the total energy of the capture cascade, E_C. Finally, Eq. 3 allows us to obtain the capture yield, where N^w is the weighted counting rate.

$$Y(E_n) = \frac{N^w(E_n)}{N_n(E_n)E_C(E_n)} \tag{3}$$

The resulting capture yield is corrected by several experimental effects such as summing, presence of conversion electrons in the radiative cascade and deposited energy threshold used for C_6D_6. In addition, this capture yield is normalized to a resonance of reference by means of the SRM [18], in order to cancel out possible disagreements between the actual experimental setup and the MC simulations made to obtain the WF.

Fig. 2 shows the neutron capture yield of ^{80}Se obtained in this work and analyzed with the SAMMY code [22]. The latter employs the R-Matrix theory to fit the capture yield resonances using the properties of the nuclear levels of the compound nucleus, such as the energy, E_0, partial widths, Γ_γ and Γ_n, and the spin-parity, J^π. In this work, a total of 113 resonances have been characterized, 98 of them for the first time and 15 previously known from transmission measurements [23]. No resonance data were known from the previous ToF neutron capture measurement [13].

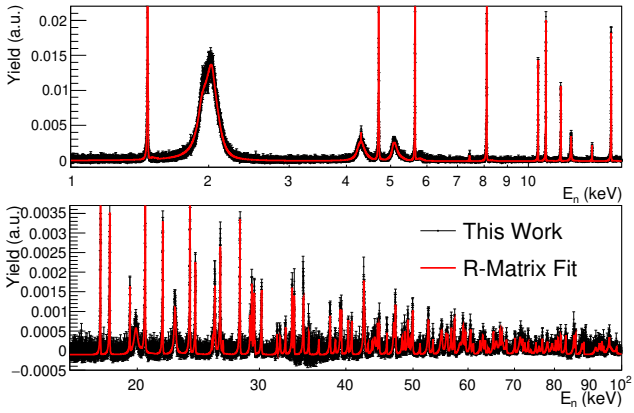

Figure 2. Experimental ^{80}Se(n, γ) yield calculated in this work in the energy range between 1 keV and 16 keV (top panel), and from 16 keV to 100 keV (bottom panel). In both panels, together with the experimental yield is presented the R-Matrix fit.

4 Neutron capture cross section of ^{80}Se

The resonance parameters, provided by the analysis described in Sec. 3, are related to the neutron capture cross section by means of Eq. 4, which was first derived by Breit and Wigner in 1936 [24],

$$\sigma_{n\gamma} = \pi \lambda\!\!\!^{-2}_n g \frac{\Gamma_n \Gamma_\gamma}{(E_n - E_0)^2 + (\Gamma/2)^2}, \tag{4}$$

where $\lambda\!\!\!^{-}_n$ is the de Broglie wave length (Eq. 5) and g is the spin factor (Eq. 6).

$$\lambda\!\!\!^{-}_n = \frac{\hbar}{2\pi} \frac{A+1}{A} \frac{1}{\sqrt{E_n}} \tag{5}$$

$$g = \frac{(2J+1)}{(2I+1)(2s+1)}. \tag{6}$$

Fig. 3 shows the neutron capture cross section of ^{80}Se obtained in this work and compared to previous data including: Previous low-resolution ToF measurement [13] and data from evaluated libraries [25, 26]. With respect to the former, the quality of the new data improves in terms of energy resolution and completeness, being able to resolve resonance structures up to 100 keV of neutron energy, as well as characterizing the low energy region below 3 keV, which contributes significantly to the study of the main s-process component. Furthermore, a noticeable reduction in the background level can be appreciated respect to the previous measurement. On the other hand, the comparison with the evaluated libraries shows discrepancies that emphasize the importance of this high resolution measurement.

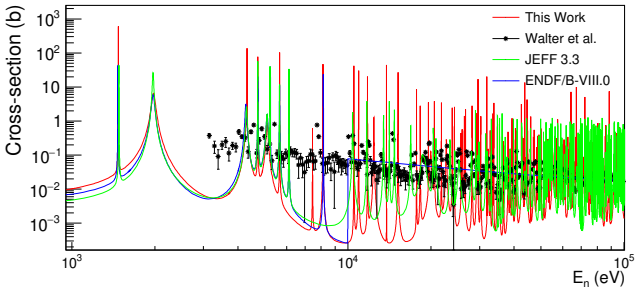

Figure 3. ^{80}Se(n, γ) cross section obtained in this work compared to previous available data as well as current evaluated cross sections.

The neutron capture cross section, $\sigma_\gamma(E_n)$, shown in Fig. 3 displays the probability of a nucleus to capture a neutron of certain kinetic energy, E_n. Since neutrons in stars follow Maxwell distribution of velocities for a given temperature, T, the Maxwellian Averaged Cross Section (MACS) is the magnitude of interest for stellar models to study the s-process. A common expression is given in Eq. 7, where k is the Stephan-Boltzmann constant.

$$\text{MACS} = \frac{2}{(kT)^2\sqrt{\pi}} \int_0^\infty \sigma_\gamma(E_n) E_n e^{-E_n/kT} dE_n \tag{7}$$

In this work, the MACS of the ^{80}Se(n, γ) reaction has been determined at stellar temperatures between 1 keV and 60 keV, and compared to previous available data, as it is shown in Fig. 4. The MACS values obtained in this work are between 20% and 40% lower compared to the previous ToF measurement [13]. This disagreement is slightly reduced but still present when comparing the new data with those available in the KADoNiS v1.0 database [27]. The high energy resolution of our n_TOF-EAR1 and the low neutron sensitivity of the setup compared to the previous experimental data set have allowed us, among others, to carry out a very precise background subtraction. Moreover, the careful application of the PHWT has enabled an accurate assessment of the detection efficiency. These factors may be responsible for the differences with the previous work.

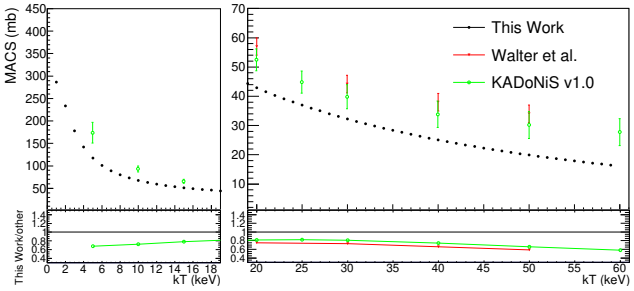

Figure 4. ^{80}Se(n, γ) MACS obtained in this work between 1 keV and 60 keV and compared to previous available data.

Finally, Tab. 3 displays the numerical values of the ^{80}Se(n, γ) MACS for three different kT values, which are close to relevant points of the s-process, and where our data can be compared to the rest of calculations. There, our MACS is 30%, 20% and 50% lower than those available in KADoNiS, which can be considered the previous state-of-the-art values. In addition, statistical uncertainties have been improved by a factor of ten in new results.

Table 3. Value of the MACS at three different stellar temperatures. Only statistical uncertainties are included in these results.

	MACS (mb)		
	at 10 keV	at 30 keV	at 90 keV
KADoNis	93.6(6.8)	39.8(4.1)	23.7(4.3)
Walter et al.	–	44(3)	–
This Work	**67.6(4)**	**32.2(3)**	**9.5(1)**

The study of the astrophysical impact of these new data will be addressed in combination with the new results from the ^{79}Se(n, γ) cross section measurement recently carried out at CERN n_TOF [28]. However, a preliminary calculation using the NETZ tool [29] shows how a 50% variation in the MACS of ^{80}Se(n, γ) induces a 60% variation on the abundance ratio of ^{80}Se itself, normalized to the abundance of this isotope before introducing the 50% change in the MACS. As well as a smaller amplitude but far-reaching propagation effect over nine heavier isotopes of Se, Br and Kr, thus impacting the reference s-only ^{80}Kr and beyond. These results highlight the relevance of this new and more precise measurement of the ^{80}Se(n, γ) cross section on the abundances of elements produced via the s-process. Therefore, in combination with new results on ^{79}Se(n, γ) MACS, the high quality data reported in this work will improve our knowledge about the s-process.

5 Acknowledgement

We acknowledge support from from the European Research Council (ERC) under the European Union's Horizon 2020 research and innovation program (grant agreement No. 681740), and the Spanish Science Ministry for funding projects FPA2017-83946-C2-1-P and PID2019-104714GB-C21. This work is part of the PhD Thesis of V. Babiano-Suarez.

References

[1] E.M. Burbidge, G.R. Burbidge, W.A. Fowler, F. Hoyle, Reviews of Modern Physics **29**, 547 (1957)
[2] A.G.W. Cameron, *Stellar evolution, nuclear astrophysics, and nucleogenesis. Second edition* (Dover Publications, 2013), originally published as a technical report by Atomic Energy of Canada, Ltd., 1957, https://www.osti.gov/biblio/4709881
[3] F. Käppeler, R. Gallino, S. Bisterzo, W. Aoki, Reviews of Modern Physics **83**, 157 (2011), 1012.5218
[4] S. Degl'Innocenti, P.G. Prada Moroni, M. Marconi, A. Ruoppo, Astrophysics and Space Science **316**, 25 (2008)
[5] B. Paxton, L. Bildsten, A. Dotter, F. Herwig, P. Lesaffre, F. Timmes, Astrophysical Journal Supplement **192**, 3 (2011)
[6] M. Pignatari, F. Herwig, R. Hirschi, M. Bennett, G. Rockefeller, C. Fryer, F.X. Timmes, C. Ritter, A. Heger, S. Jones et al., Astrophysical Journal Supplement **225**, 24 (2016)
[7] R. Gallino, C. Arlandini, M. Busso, M. Lugaro, C. Travaglio, O. Straniero, A. Chieffi, M. Limongi, The Astrophysical Journal **497**, 388 (1998)
[8] F. Käppeler, Progress in Particle and Nuclear Physics **43**, 419 (1999)
[9] G. Jörg, R. Bühnemann, S. Hollas, N. Kivel, K. Kossert, S. Van Winckel, C.L.v. Gostomski, Applied Radiation and Isotopes **68**, 2339 (2010)
[10] U. Ott, F. Begemann, J. Yang, S. Epstein, Nature **332**, 700 (1988)
[11] V. Babiano-Suárez, L. Caballero, C. Domingo-Pardo, C. Guerrero, A. Tarifeño-Saldivia, Tech. Rep. CERN-INTC-2018-005, INTC-P-536, CERN, Geneva (2018), http://cds.cern.ch/record/2299660
[12] High-sensitivitY Measurements of key stellar Nucleo-Synthesis reactions (HYMNS), ERC-consolidator grant agreement no. 681740, PI: C. Domingo Pardo.
[13] G. Walter, H. Beer, F. Kaeppeler, G. Reffo, F. Fabbri, Astronomy and Astrophysics **167**, 186 (1986)
[14] C. Guerrero, A. Tsinganis, E. Berthoumieux, M. Barbagallo, F. Belloni, F. Gunsing, C. Weiß, E. Chiaveri, M. Calviani, V. Vlachoudis et al., European Physical Journal A **49**, 27 (2013)
[15] R. Plag, M. Heil, F. Käppeler, P. Pavlopoulos, R. Reifarth, K. Wisshak, n TOF Collaboration, Nuclear Instruments and Methods in Physics Research A **496**, 425 (2003)
[16] P.F. Mastinu, R. Baccomi, E. Berthoumieux, D. Cano-Ott, F. Gramegna, C. Guerrero, C. Massimi, P.M. Milazzo, F. Mingrone, J. Praena et al., Tech. Rep. CERN-INTC-2013-002, CERN (2013)

[17] C. Domingo-Pardo, U. Abbondanno, G. Aerts, H. Álvarez-Pol, F. Alvarez-Velarde, S. Andriamonje, J. Andrzejewski, P. Assimakopoulos, L. Audouin, G. Badurek et al., Physical Review C **74**, 055802 (2006), nucl-ex/0610039

[18] R.L. Macklin, J. Halperin, R.R. Winters, Nuclear Instruments and Methods **164**, 213 (1979)

[19] U. Abbondanno, G. Aerts, H. Alvarez, S. Andriamonje, A. Angelopoulos, P. Assimakopoulos, C.O. Bacri, G. Badurek, P. Baumann, F. Bečvář et al., Nuclear Instruments and Methods in Physics Research A **521**, 454 (2004)

[20] J. Allison, K. Amako, J. Apostolakis, H. Araujo, P.A. Dubois, M. Asai, G. Barrand, R. Capra, S. Chauvie, R. Chytracek et al., IEEE Transactions on Nuclear Science **53**, 270 (2006)

[21] J. Allison, K. Amako, J. Apostolakis, P. Arce, M. Asai, T. Aso, E. Bagli, A. Bagulya, S. Banerjee, G. Barrand et al., Nuclear Instruments and Methods in Physics Research A **835**, 186 (2016)

[22] N.M. Larson, ORNL/TM-9179/R8, Oak Ridge National Laboratory, Oak Ridge, TN (2008)

[23] G.M. Novoselov, V.G. Krivenko, L.L. Litvinskij, I.M. Simonov, Jadernye Konstanty (Nuclear Constants) **1-2**, 3 (1995)

[24] G. Breit, E. Wigner, Physical Review **49**, 519 (1936)

[25] D.A. Brown, M.B. Chadwick, R. Capote, A.C. Kahler, A. Trkov, M.W. Herman, A.A. Sonzogni, Y. Danon, A.D. Carlson, M. Dunn et al., Nuclear Data Sheets **148**, 1 (2018)

[26] A.J.M. Plompen, O. Cabellos, C. De Saint Jean, M. Fleming, A. Algora, M. Angelone, P. Archier, E. Bauge, O. Bersillon, A. Blokhin et al., European Physical Journal A **56**, 181 (2020)

[27] I. Dillmann, T. Szücs, R. Plag, Z. Fülöp, F. Käppeler, A. Mengoni, T. Rauscher, Nuclear Data Sheets **120**, 171 (2014)

[28] V. Babiano-Suárez, J. Balibrea-Correa, L. Caballero, F. Calviño, D. Cano-Ott, A. Casanovas, N. Colonna, S. Cristallo, C. Domingo-Pardo, C. Guerrero et al., Tech. Rep. CERN-INTC-2020-065, INTC-P-580, CERN, Geneva (2020), http://cds.cern.ch/record/2731962

[29] M. Weigand, T.A. Bredeweg, A. Couture, K. Göbel, T. Heftrich, M. Jandel, F. Käppeler, C. Lederer, N. Kivel, G. Korschinek et al., Physical Review C **92**, 045810 (2015), 1512.02263